Crystallographic Studies with Xenon and Nitrous Oxide Provide Evidence for Protein-dependent Processes in the Mechanisms of General Anesthesia

Jacques H. Abraini, Ph.D., D.Sc., Psy.D., Guillaume Marassio, Ph.D., Helene N. David, Ph.D., Beatrice Vallone, Ph.D., D.Sc., Thierry Prangé, Ph.D., D.Sc., Nathalie Colloc'h, Ph.D., D.Sc.

ABSTRACT

Background: The mechanisms by which general anesthetics, including xenon and nitrous oxide, act are only beginning to be discovered. However, structural approaches revealed weak but specific protein–gas interactions.

Methods: To improve knowledge, we performed x-ray crystallography studies under xenon and nitrous oxide pressure in a series of 10 binding sites within four proteins.

Results: Whatever the pressure, we show (1) hydrophobicity of the gas binding sites has a screening effect on xenon and nitrous oxide binding, with a threshold value of 83% beyond which and below which xenon and nitrous oxide, respectively, binds to their sites preferentially compared to each other; (2) xenon and nitrous oxide occupancies are significantly correlated respectively to the product and the ratio of hydrophobicity by volume, indicating that hydrophobicity and volume are binding parameters that complement and oppose each other's effects; and (3) the ratio of occupancy of xenon to nitrous oxide is significantly correlated to hydrophobicity of their binding sites.

Conclusions: These data demonstrate that xenon and nitrous oxide obey different binding mechanisms, a finding that argues against all unitary hypotheses of narcosis and anesthesia, and indicate that the Meyer–Overton rule of a high correlation between anesthetic potency and solubility in lipids of general anesthetics is often overinterpreted. This study provides evidence that the mechanisms of gas binding to proteins and therefore of general anesthesia should be considered as the result of a fully reversible interaction between a drug ligand and a receptor as this occurs in classical pharmacology. **(ANESTHESIOLOGY 2014; 121:1018-27)**

THE mechanisms by which general anesthetics, including the remarkably safe medicinal gases xenon and nitrous oxide, produce their pharmacological action are still poorly known. However, over the past 15 yr, major progress has been made with regard to the molecular mechanisms by which xenon and nitrous oxide act to produce their anesthetic and neuroprotective effects.[1–11] In contrast with most inhalational clinical anesthetics thought to act by potentiating the type A γ-aminobutyric acid receptor, xenon and nitrous oxide have been shown to act mainly by antagonizing the *N*-methyl-D-aspartate glutamatergic receptor[2,9,12–14] and by modulating other neuronal targets of physiological and clinical interest such as the nicotinic acetylcholine receptor, the TREK-1 two-pore–domain K^+ channel, and enzymes.[14–18]

Crystallographic studies under gas pressure have allowed a better understanding of the mechanisms by which the chemically and metabolically inert gases act, particularly by demonstrating in protein models of possible neuronal targets that such gases bind to proteins through weak but specific interactions[19–26] within hydrophobic cavities and/or surface pockets. In that way, recent investigations have further

What We Already Know about This Topic

- Hydrophobicity is often considered to be the principal physicochemical property determining gas binding to proteins
- Chemically and metabolically inert gases bind to proteins through weak, but specific, interactions within hydrophobic cavities and surface pockets

What This Article Tells Us That Is New

- Crystallographic studies of 10 binding sites in 4 proteins found that the binding of xenon and nitrous oxide do not depend on hydrophobicity alone but on complex processes in which hydrophobicity and volume interact in different ways
- Gas, including general anesthetic, binding to proteins should be considered to be due to a fully reversible interaction between a ligand and a receptor

Supplemental Digital Content is available for this article. Direct URL citations appear in the printed text and are available in both the HTML and PDF versions of this article. Links to the digital files are provided in the HTML text of this article on the Journal's Web site (www.anesthesiology.org).

Submitted for publication January 17, 2014. Accepted for publication August 12, 2014. From the Faculté de Médecine, Université de Caen Basse Normandie, Normandie-Université, Caen, France (J.H.A., G.M.); Institut de Recherche Biomédicale des Armées, Brétigny-sur-Orge, France (J.H.A.); Département d'Anesthésiologie, Université Laval, Quebec City, Québec, Canada (J.H.A., H.N.D.); Centre de Recherche Hôtel-Dieu de Lévis, CSSS Alphonse-Desjardins, Lévis, Québec, Canada (H.N.D.); Department of Biochemical Sciences, University of Rome La Sapienza, Rome, Italy (B.V.); LCRB UMR 8015, Université Paris Descartes–CNRS, Faculté de Pharmacie, Paris, France (T.P.); ISTCT UMR 6301, CNRS, CERVOxy group, GIP Cyceron, Caen, France (N.C.); ISTCT UMR 6301, Université de Caen Basse Normandie, Normandie-Université, Caen, France (N.C.); and ISTCT UMR 6301, CEA DSV/I2BM, Caen, France (N.C.).

 Anesthesiology 2014; 121:1018-27

shown that xenon and nitrous oxide bind to and compete for the same hydrophobic sites.[18,19]

In the present study, we performed crystallography studies in a series of four proteins—urate oxidase, lysozyme, myoglobin, and neuroglobin—to better understand the basic mechanisms that determine xenon and nitrous oxide binding to proteins. We confirmed that xenon and nitrous oxide bind in most cases to the same binding sites and further demonstrated mainly that the binding of xenon and nitrous oxide to proteins does not depend on hydrophobicity alone but on complex processes in which hydrophobicity and volume interact in different ways.

Materials and Methods

Crystal Preparations

Urate oxidase (EC = 1.7.3.3; uricase) is a homotetrameric enzyme of 135 kDa that catalyzes the oxidation of uric acid. Purified recombinant urate oxidase from *Aspergillus flavus*, expressed in *Saccharomyces cerevisiae*, was provided by Sanofi-Aventis (Montpellier, France). Urate oxidase crystals were grown by the batch or hanging drop techniques at room temperature using a 10–15 mg/ml solution of urate oxidase with an excess of its inhibitor 8-azaxanthine (Sigma-Aldrich, Lyon, France) in 50 mM Tris/HCl pH 8.5 in the presence of 5–8% polyethylene glycol 8000. This led to crystals in orthorhombic space group I222 with one monomer per asymmetric unit.[27]

Hen egg white lysozyme (E.C. 3.2.1.17) is a monomeric enzyme of 15 kDa that hydrolyzes specific linkages in peptidoglycans. Purified lysozyme was purchased from Hampton Research (Aliso Viejo, CA) and dissolved in sodium acetate buffer 0.02 M pH 4.6. Lysozyme crystals were grown by the batch technique using a 15–30 mg/ml solution of lysozyme in 0.1 M sodium acetate buffer, pH 4.6, in the presence of 0.6 to 1.1 M NaCl. This led to crystals in the tetragonal space group $P4_32_12$ with one enzyme per asymmetric unit.[28]

Sperm whale myoglobin is a monomeric globin of 19 kDa involved in oxygen storage by reversibly binding oxygen molecules that have been transported by hemoglobin. Myoglobin crystals were grown by the batch technique by mixing 50 mg/ml myoglobin in 50 mM potassium phosphate buffer, pH 7, and saturated ammonium sulfate. This led to crystals in the monoclinic space group $P2_1$ with one globin per asymmetric unit.[29]

Murine neuroglobin is a hexacoordinate globin of 18 kDa expressed in the brain of vertebrates, which is involved in neuroprotection during hypoxia and ischemia.[30–32] Neuroglobin production, purification, and crystallization have been described previously.[33] Crystals grew in a 1:1 mixture of neuroglobin (10 mg/ml) and reservoir solution (1.6 M ammonium sulfate, 0.1 M morpholino-ethanesulfonic acid, pH 6.5) in the hanging-drop method. This led to neuroglobin crystals in the trigonal space group R32 with one globin per asymmetric unit.

Data Collections

Data collections were recorded gas-less and under gas pressure of xenon or nitrous oxide of 10, 20, and 30 bar. For each data collection, a crystal mounted in a quartz capillary fitted to a specially designed cell was pressurized and maintained under gas pressure as described earlier.[34,35] Diffraction data were collected at room temperature at the BM14, BM16, and BM30A beamlines at the European Synchrotron Radiation Facility in Grenoble, France. Detectors used were a MAR CCD detector for BM14, an ADSC Q210r CCD detector for BM16, and an ADSC Q315r CCD detector for BM30A. Data were indexed and integrated by *DENZO* and scaled independently and reduced using *SCALEPACK*, both programs from the *HKL* package[36] or indexed and integrated by *MOSFLM*[37] and scaled by *SCALA*. Intensities were converted in structure factor amplitudes using *TRUNCATE*, and structure refinements were carried out using *REFMAC*,[38] all from the *CCP4* package.[39] Protein Data Bank entries 2IBA for urate oxidase,[19] 1C10 for lysozyme,[23] 2JHO for myoglobin,[40] and 3GKT for neuroglobin[21] in which heteroatoms and alternate side-chain positions were removed were used as starting model for rigid body refinement. The graphics program *COOT*[41] was used to visualize $|2F_{obs} - F_{calc}|$ and $|F_{obs} - F_{calc}|$ electron density maps and for manual rebuilding. All data collections were made at wavelength in the range 0.95–1 Å far from the xenon K-edge (0.3587 Å) or LI-edge (2.2738 Å) restraining the use of xenon anomalous signal to accurately determine occupancies in xenon complexes. However, with a residual of 3 to 4 electrons, the $\Delta f''$ signal was enough to assess the presence of xenon from peaks in anomalous difference maps.[18] Determination of gas occupancies have been deduced, as in Reference 18, from the height of the peaks corresponding to the gas in the omit maps. The resulting gas B-factors were constant for a given binding site whatever the applied gas pressure. Hydrophobicity of the gas binding site has been estimated by calculating the percentage of carbon atoms in the total number of atoms (carbon, oxygen, nitrogen, and sulfur, ignoring hydrogen) that line the binding site. Cavity and pocket volumes were calculated using the program CASTp[42] with a probe radius of 1.4 Å. Summary of the x-ray data collections and refinements statistics for each sample is reported in Supplemental Digital Content 1, http://links.lww.com/ALN/B90. Atomic coordinates and structure factors have been deposited in the Protein Data Bank (4NWH lysozyme under 30 bar of xenon, 4NWE lysozyme under 30 bar of nitrous oxide, 4NXA myoglobin under 30 bar of xenon, 4NXC myoglobin under 30 bar of nitrous oxide, 4O4T for neuroglobin under 30 bar of xenon, and 4O4Z for neuroglobin under 30 bar of nitrous oxide).

Data Modeling and Statistical Analysis

Raw data of binding site occupancies by xenon and nitrous oxide were modeled *versus* pressure using the Origin8 software (OriginLab, Northampton, MA) according to the following logistic equation:

$$Y = \frac{y_1 - y_2}{1 + (X / x_0)^p} + y_2 \quad (1)$$

where y_1 is the lower (or initial) experimental value, y_2 the higher (or final) experimental value, x_0 the x-axis value that corresponds to the y-axis value $y_0 = y_1 + (y_2 - y_1)/2$, and p the power of the sigmoidal fit (fixed to 3). Then, the dose–response occupancies of xenon and nitrous oxide as defined by the predicted values of occupancy obtained from equation (1) were compared by performing a Poisson analysis for distribution.

The relationships between the predicted values of occupancy of xenon and nitrous oxide were modeled *versus* the gas binding sites' hydrophobicity and volume, as well as their product and ratio, using equation (1). The level of statistical significance for the Poisson analysis and the r values obtained from equation (1) was set at P less than 0.05.

Results

Xenon and Nitrous Oxide Binding

Xenon and nitrous oxide bound to hydrophobic sites by either intramolecular cavities or solvent-accessible pockets. As an example, figure 1 illustrates the binding of xenon and nitrous oxide to lysozyme (fig. 1A), myoglobin (fig. 1B), and neuroglobin (fig. 1C). As reported previously,[34,43] the presence of xenon or nitrous oxide in the binding sites did not change unit cell parameters and only had little effect on the proteins structure (root mean square differences between native structures and structures with gas were about 0.2 Å for all protein atoms). As already reported,[18,19] the only gas-induced structural effect was a dose (pressure)-dependent expansion of the volume of the gas binding site that did not result, however, in an increase of the number of xenon and nitrous oxide atoms within the gas binding sites.

Urate Oxidase. As reported previously,[18,19] we found that xenon and nitrous oxide bound to urate oxidase within an internal cavity, called UOX-I, located close to the active site of urate oxidase. UOX-I has 90% of lining atoms that are carbons. In the gas-less structure of urate oxidase, UOX-I is empty and has a volume of 116 Å^3. Xenon and nitrous oxide bound to UOX-I in a pressure-dependent manner of 10 to 30 bar (fig. 2A). Statistical analysis showed a significant difference between xenon and nitrous oxide occupancy of UOX-I ($Z = 4.34$, $P < 0.001$), indicating that xenon has a higher affinity than nitrous oxide for UOX-I.

Xenon and nitrous oxide also bound weakly to a small extension of a preexisting pocket, called UOX-II, previously suggested to be not involved in the enzymatic activity of urate oxidase[18] and further shown to be a negligible factor in a mechanistic model of anesthesia based on xenon and nitrous oxide *in vivo* pharmacology and crystallography data.[19] Therefore, this gas binding site was not taken into account in our analysis.

Lysozyme. As described previously,[23,44,45] we found that xenon bound to lysozyme within a small buried internal cavity, called LYSO-I (fig. 1A). LYSO-I is a "full" hydrophobic cavity with 100% of lining atoms being carbons. In the gas-less structure of lysozyme, LYSO-I is empty and has a volume of 32 Å^3. Xenon bound to LYSO-I in a pressure-dependent manner of 10 to 30 bar; nitrous oxide did not bind to LYSO-I (fig. 2B). This led to a significant difference between xenon and nitrous oxide occupancy ($Z = 6.56$, $P < 0.001$).

Also, xenon and nitrous oxide bound to a second pocket called LYSO-II located at a crystallographic interface, a condition indicating that this site is an experimental artifact. Therefore, this gas binding site was not taken into account in our analysis.

Myoglobin. In agreement with previous observation,[46–48] we found that xenon bound to myoglobin within four binding sites, called MB-I to MB-IV (fig. 1B). Here, we further showed that xenon also bound to an additional site, called MB-V, and that nitrous oxide bound to the same sites as xenon. MB-III and MB-V are with no doubt internal cavities. Likewise, if the heme is taken as being an intrinsic part of the globin, MB-I, MB-II, and MB-IV can be considered as internal cavities buried between the heme and the globin.

MB-I is located on the proximal side of the heme and has 83% of lining atoms that are carbons. In the gas-less

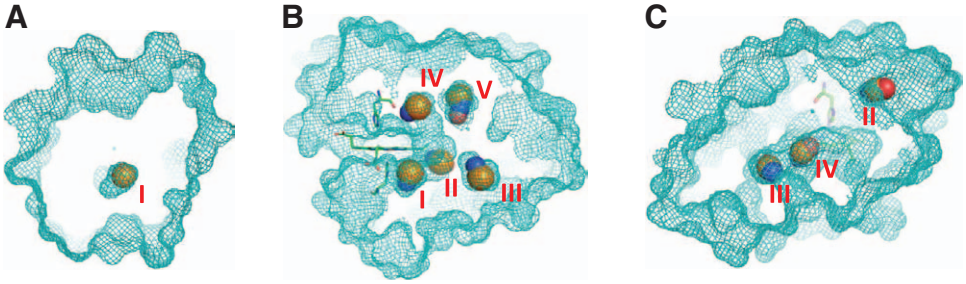

Fig. 1. Xenon and nitrous oxide binding sites in lysozyme (*A*), myoglobin (*B*), and neuroglobin (*C*). Xenon is represented by an *orange* sphere, nitrous oxide is represented by spheres colored by atom types, and protein surfaces are represented as mesh volumes in *cyan*. The heme and the proximal and distal histidines are represented in stick colored by atom types in the myoglobin and neuroglobin structures (*B* and *C*).

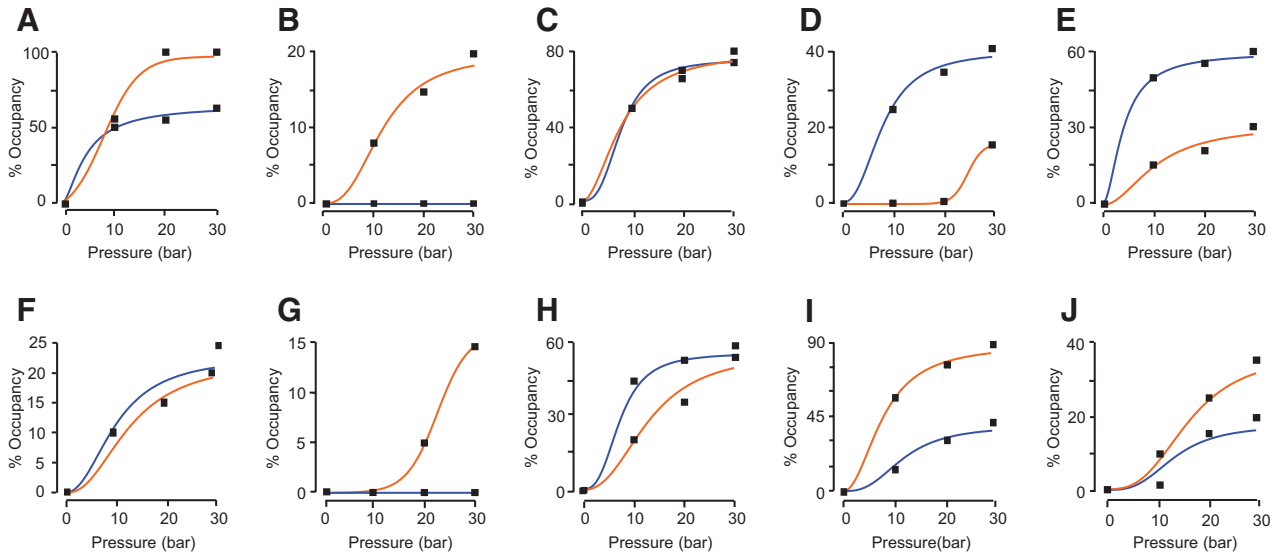

Fig. 2. Occupancy of the gas binding sites by xenon and nitrous oxide as a function of pressure. (*A*) Urate oxidase, UOX-I, (*B*) lysozyme, LYSO-I, (*C*) myoglobin, MB-I, (*D*) myoglobin, MB-II, (*E*) myoglobin, MB-III, (*F*) myoglobin, MB-IV, (*G*) myoglobin, MB-V, (*H*) neuroglobin, NGB-II, (*I*) neuroglobin, NGB-III, and (*J*) neuroglobin, NGB-IV. Statistical analysis showed a significant difference between xenon and nitrous oxide occupancy of UOX-I, LYSO-I, MB-II, MB-III, MB-V, NGB-II, NGB-III, and NGB-IV, but not between xenon and nitrous oxide occupancy of MB-I and MB-IV. *Orange lines*: xenon (Xe); *blue lines*: nitrous oxide (N_2O). UOX-I: binding site no. 1 in urate oxidase; LYSO-I: binding site no. 1 in lysozyme; MB-I, MB-II, MB-III, MB-IV, and MB-V: binding sites nos. 1 to 5 in myoglobin; NGB-II, NGB-III, and NGB-IV: binding sites nos. 2 to 4 in neuroglobin. Y-axis: occupancy of the gas binding sites by xenon and nitrous oxide as expressed in %; X-axis: pressure of gas expressed in bar (1 bar = 0.1 MPa).

structure of myoglobin, MB-I is empty and has a volume of 66 Å^3. Xenon and nitrous oxide bound to MB-I in a pressure-dependent manner of 10 to 30 bar (fig. 2C). No significant difference was found between xenon and nitrous oxide occupancy of MB-I (Z = 0.00, $P < 1$), indicating that both gases have a similar affinity for MB-I.

MB-II is located close to the heme and possesses 73% of lining atoms that are carbons. In the gas-less structure of myoglobin, MB-II is empty and has a volume of 42 Å^3. Xenon and nitrous oxide bound to MB-II in a pressure-dependent manner of 10 to 30 bar (fig. 2D). Statistical analysis resulted in a significant difference between nitrous oxide and xenon occupancy of MB-II ($Z = -7.93$, $P < 0.001$), indicating that nitrous oxide has a higher affinity than xenon for MB-II.

MB-III has 59% of lining atoms that are carbons. In the gas-less structure of myoglobin, MB-III is filled with a water molecule and has a volume of 74 Å^3. Xenon and nitrous oxide bound to MB-III in a pressure-dependent manner of 10 to 30 bar (fig. 2E). Statistical analysis showed a significant difference between nitrous oxide and xenon occupancy of MB-III (Z = –6.59, $P < 0.001$), indicating that nitrous oxide has a higher affinity than xenon for MB-III.

MB-IV is located on the distal side of the heme and has 83% of lining atoms that are carbons. In the gas-less structure of myoglobin, MB-IV is empty and has a volume of 40 Å^3. Both xenon and nitrous oxide bound to MB-IV in a pressure-dependent manner of 10 to 30 bar (fig. 2F). Statistical analysis revealed no significant difference between xenon and nitrous oxide occupancy of MB-IV ($Z = 0.51$, $P < 0.7$), a result indicating that xenon and nitrous oxide have a similar affinity for MB-IV.

MB-V has 93% of lining atoms that are carbons. In the gas-less structure of myoglobin, MB-V is empty and has a volume of 35 Å^3. Xenon bound to MB-V in a pressure-dependent manner of 10 to 30 bar (fig. 2G); nitrous oxide did not bind to MB-V. This led to a significant difference between xenon and nitrous oxide occupancy ($Z = 4.47$, $P < 0.001$).

Neuroglobin. A large internal cavity is located behind the heme and is involved in the heme sliding mechanism in neuroglobin.[33,49] We found that xenon bound to neuroglobin within four binding sites called NGB-I to NGB-IV as reported previously[21] and to three additional sites called NGB-V to NGB-VII (fig. 1C). Nitrous oxide bound to the same sites as xenon, except NGB-V and NGB-VII.

NGB-I, NGB-V, NGB-VI, and NGB-VII are located in crystallographic interfaces, indicating that these sites are experimental artifacts. Therefore, these sites were not taken into account in our analysis.

NGB-II is a solvent-accessible pocket with 72% of lining atoms being carbons. In the gas-less structure, NGB-II is empty with a volume of 51 Å^3. Xenon and nitrous oxide bound to NGB-II in a pressure-dependent manner of 10 to 30 bar (fig. 2H). Statistical analysis showed a significant difference between nitrous oxide and xenon occupancy of NGB-II ($Z = -3.04$, $P < 0.005$), indicating that nitrous oxide has a higher affinity for NGB-II than xenon.

NGB-III is located at the back of the large internal cavity, close to a tunnel connecting the heme cavity to the exterior of the protein, and thought to be a secondary access for oxygen.[21,50] NGB-III has 86% of lining atoms being carbons. In the gas-less structure, NGB-III is empty and has a volume of 62 Å^3. Xenon and nitrous oxide bound to NGB-III in a pressure-dependent manner of 10 to 30 bar (fig. 2I). Statistical analysis showed a significant difference between xenon and nitrous oxide occupancy of NGB-III ($Z = 7.73$, $P < 0.001$), indicating that xenon has a higher affinity for NGB-III than nitrous oxide.

NGB-IV is also located in the large internal cavity, between the heme and NGB-III, with 89% of lining atoms being carbons. In the gas-less structure, NGB-IV is empty with a volume of 55 Å^3. Xenon and nitrous oxide bound to NGB-IV in a pressure-dependent manner of 10 to 30 bar (fig. 2J). Statistical analysis showed a significant difference between xenon and nitrous oxide occupancy of NGB-IV ($Z = 3.42$, $P = 0.001$), indicating that xenon has a higher affinity for NGB-IV than nitrous oxide.

Taken together, these data confirm and extend previous studies that have first shown in two intramolecular binding cavities that xenon and nitrous oxide bind to and compete for the same binding sites.[18,19]

Relationships between Occupancy, Hydrophobicity, and Volume of the Gas Binding Sites

As shown in figure 3, it is obvious that (1) xenon bound with a higher occupancy than nitrous oxide in the binding sites whose lining atoms include more than 83% of carbon atoms; (2) nitrous oxide bound with a higher occupancy than xenon in the binding sites whose lining atoms include less than 83% of carbon atoms; (3) xenon and nitrous oxide bound with a similar affinity to the binding sites whose lining atoms include 83% of carbon atoms.

Whatever the pressure (10, 20, or 30 bar), occupancy of the gas binding sites by xenon showed a significant logistic relationship with the gas binding site's volume (10 bar: $r = 0.7798$, $P < 0.01$, $df = 8$; 20 bar: $r = 0.784$, $P < 0.01$, $df = 8$; 30 bar: $r = 0.778$, $P < 0.01$, $df = 8$) but not with the gas binding site's hydrophobicity ($r = 0.000$, $P = 1$) (data not shown). Likewise, occupancy of the gas binding sites by nitrous oxide showed a significant logistic relationship with the gas binding site's volume (10 bar: $r = 0.727$, $P < 0.02$, $df = 8$; 20 bar: $r = 0.778$, $P < 0.01$, $df = 8$; 30 bar: $r = 0.792$, $P < 0.01$, $df = 8$) but not with the gas binding site's hydrophobicity ($0.591 < r < 0.621$, $P < 0.1$) (data not shown). In addition, because both hydrophobicity and volume play a critical role in gas binding to proteins, we further examined possible interactions between these factors. Occupancy by xenon of the gas binding sites showed a higher significant logistic relationship with the product of hydrophobicity by volume (10 bar: $r = 0.910$, $P < 0.001$, $df = 8$, fig. 4A; 20 bar: $r = 0.909$, $P < 0.001$, $df = 8$, fig. 4B; 30 bar: $r = 0.897$, $P < 0.001$, $df = 8$, fig. 4C) compared to the ratio of hydrophobicity to volume (10 bar: $r = 0.612$, $P < 0.1$, $df = 8$; 20 bar: $r = 0.647$, $P < 0.05$, $df = 8$; 30 bar: $r = 0{,}620$, $P < 0.1$, $df = 8$; data not shown). By contrast, occupancy of the gas binding sites by nitrous oxide resulted in a significant logistic relationship with the ratio of hydrophobicity to volume (10 bar: $r = 0.861$, $P < 0.005$, $df = 8$, fig. 5A; 20 bar: $r = 0.885$, $P < 0.001$, $df = 8$, fig. 5B; 30 bar: $r = 0.898$, $P < 0.001$, $df = 8$, fig. 5C), but not with the product of hydrophobicity by volume ($0.357 < r < 0.497$, $0.2 < P < 0.9$; data not shown).

Alternatively, we further found that the ratio of xenon to nitrous oxide occupancy of the gas binding sites decreased from 1.47 at 10 bar to 1.21 at 30 bar, and further showed whatever the pressure a significant logistic relationship with the gas binding sites' hydrophobicity (10 bar: $r = 0.960$, $P < 0.001$, $df = 5$, fig. 6A; 20 bar: $r = 0.984$, $P < 0.001$, $df = 5$, fig. 6B; 30 bar: $r = 0.862$, $P < 0.005$, $df = 6$, fig. 6C).

Discussion

This research was designed to better understand the mechanisms of gas binding to proteins, particularly the role of the binding sites' hydrophobicity and volume. By performing crystallography studies with xenon and nitrous oxide, we confirmed that these gases bind in most cases to the same binding sites and further showed that the binding of these gases to proteins does not depend on hydrophobicity alone but on complex processes in which hydrophobicity and volume interact in different ways.

All experiments were performed at 10, 20, and 30 bar of gas pressure, which are pressures at least 10-fold that required to obtain *in vivo* narcotic/anesthetic effects[2] and *in vitro* inhibitory effects of enzyme activity.[15,17,18,51] The relevance of such pressures to the pressure (concentration) used in clinical anesthesia could therefore be questioned. It is a well-known condition, due to slow gas penetration in crystalline systems, that the gas pressure to be used in crystallography studies must be at least 10 times higher the gas physiological concentration to allow approximating gas binding saturation in a reasonable time period.[52] In addition, the possibility that these pressures could have biased our findings should also be discussed since these are pressures under which the phenomenon of pressure reversal of anesthesia may occur. Crystallography studies with helium, an inert gas that virtually possesses no narcotic action and can therefore be considered to mediate the effect of pressure *per se*,[53] have found no effect on the structure of urate oxidase at pressures up to 45 bar.[18] In addition, studies with urate oxidase have further demonstrated that hydrostatic pressures higher than 1,000 bar are required to induce structural changes mainly characterized by compression of the gas binding sites.[54] Interestingly, such pressures are also approximately 10-fold higher than the physiological pressure at which seizures occurred in mammals[55] as the ultimate manifestation before death of the high pressure neurological syndrome, a set of excitatory symptoms whose main characteristics oppose those of

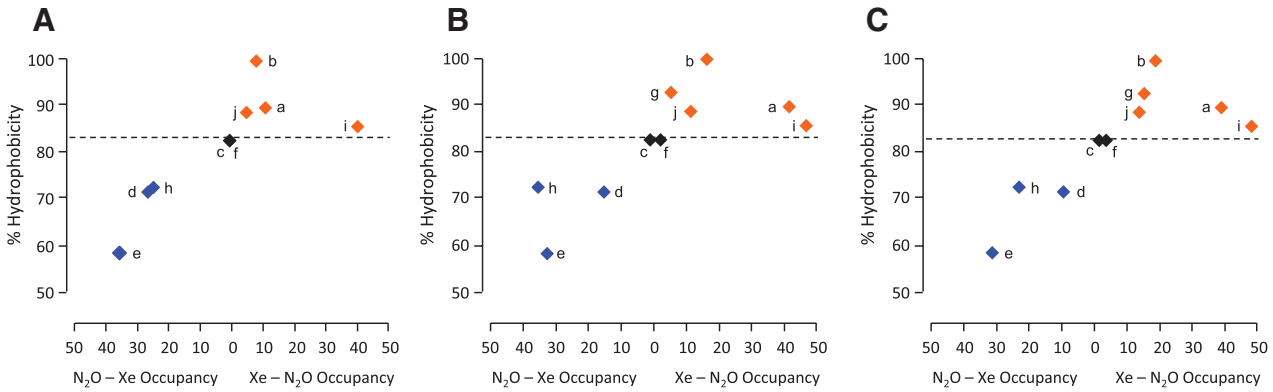

Fig. 3. Screening effects of hydrophobicity on the binding of xenon (Xe) and nitrous oxide (N_2O). (*A*) 10 bar; (*B*) 20 bar; and (*C*) 30 bar. Whatever the pressure, xenon bound with a higher occupancy than nitrous oxide in binding sites whose hydrophobicity is more than 83% (*orange diamonds*); nitrous oxide bound with a higher occupancy than xenon in binding sites whose hydrophobicity is less than 83% (*blue diamonds*); xenon and nitrous oxide bound with equal occupancy in binding sites whose hydrophobicity is 83% (*black diamonds*). These data indicate that hydrophobicity has a screening effect on xenon and nitrous oxide binding to proteins with a threshold value of 83% beyond and below which xenon and nitrous oxide binds preferentially compared to each other. *a*: Urate oxidase, UOX-I; *b*: lysozyme, LYSO-I; *c*: myoglobin, MB-I; *d*: myoglobin, MB-II; *e*: myoglobin, MB-III; *f*: myoglobin, MB-IV; *g*: myoglobin, MB-V; *h*: neuroglobin, NGB-II; *i*: neuroglobin, NGB-III; *j*: neuroglobin, NGB-IV. UOX-I: binding site no. 1 in urate oxidase; LYSO-I: binding site no. 1 in lysozyme; MB-I, MB-II, MB-III, MB-IV, and MB-V: binding sites nos. 1 to 5 in myoglobin; NGB-II, NGB-III, and NGB-IV: binding sites nos. 2 to 4 in neuroglobin. Y-axis: hydrophobicity as calculated for each protein in % of lining atoms being carbon atoms; X-axis: difference in binding to proteins between xenon and nitrous oxide.

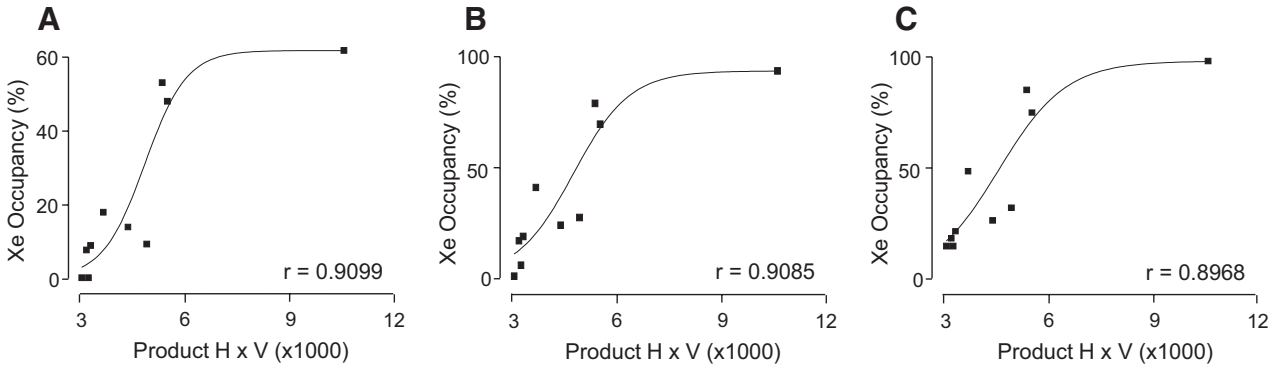

Fig. 4. Occupancy of the gas binding sites by xenon. Occupancy of the gas binding sites by xenon showed a significant logistic relationship with the product of hydrophobicity (H) by volume (V). (*A*) 10 bar, $r = 0.910$ ($r^2 = 0.828$); (*B*) 20 bar, $r = 0.909$ ($r^2 = 0.825$); and (*C*) 30 bar, $r = 0.897$ ($r^2 = 0.804$). Y-axis: xenon (Xe) occupancy of the gas binding sites as expressed in %; X-axis: the product of hydrophobicity (%) by volume (Å^3).

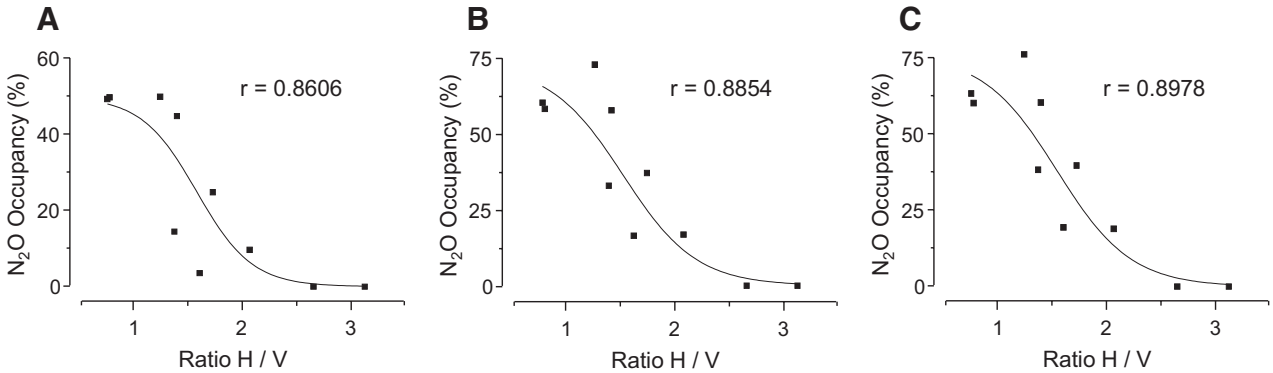

Fig. 5. Occupancy of the gas binding sites by nitrous oxide. Occupancy of the gas binding sites by nitrous oxide showed a significant logistic relationship with the ratio of hydrophobicity (H) to volume (V). (*A*) 10 bar, $r = 0.861$ ($r^2 = 0.741$); (*B*) 20 bar, $r = 0.885$ ($r^2 = 0.784$); and (*C*) 30 bar, $r = 0.898$ ($r^2 = 0.806$). Y-axis: nitrous oxide (N_2O) occupancy of the gas binding sites as expressed in %; X-axis: the ratio of hydrophobicity (%) to volume (Å^3).

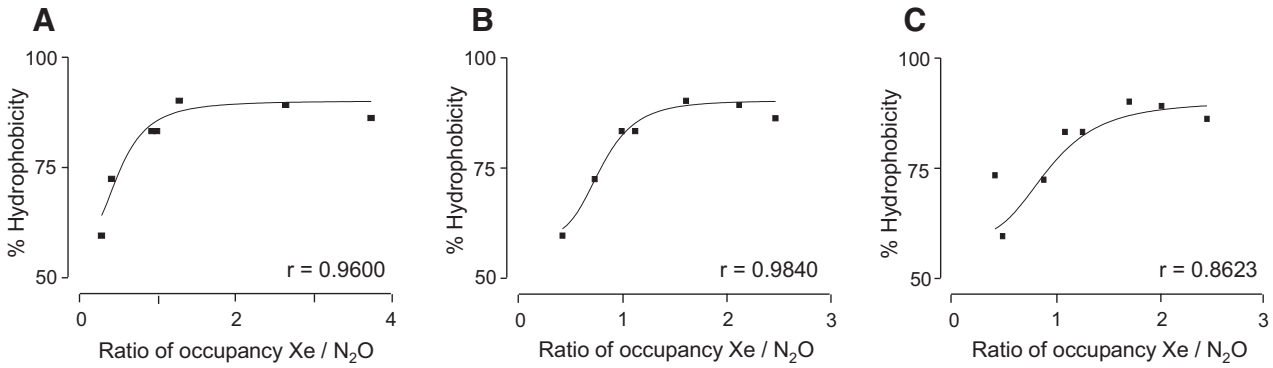

Fig. 6. Ratio of occupancy of xenon to nitrous oxide. The ratio of occupancy of the gas binding sites of xenon to nitrous oxide showed a significant logistic relationship with the binding sites' hydrophobicity. (*A*) 10 bar, $r = 0.960$ ($r^2 = 0.922$); (*B*) 20 bar, $r = 0.984$ ($r^2 = 0.968$); and (*C*) 30 bar, $r = 0.862$ ($r^2 = 0.744$). Y-axis: hydrophobicity as calculated for each protein in % of lining atoms being carbon atoms; X-axis: ratio of occupancy of xenon (Xe) to nitrous oxide (N_2O).

inert gas narcosis.[56] Alternatively, one could also question as to whether soluble proteins are good models of membrane proteins, the actual targets of inert gases and volatile anesthetics. For instance, apoferritin has been used as a model for the type A γ-aminobutyric acid receptor.[57,58] Also, there is evidence that membrane proteins such as the *Gloeobacter violaceus* and *Erwinia chrysanthemi* pentameric ligand-gated ion channels possess anesthetic binding sites similar to those found in globular proteins that are hydrophobic pockets or cavities of various sizes. In the *E. chrysanthemi* channel, xenon bound to a hydrophobic cavity within the pore,[59] and bromoform has multiple hydrophobic binding sites.[60] In the *G. violaceus* channel, general anesthetics bound to a large intramolecular hydrophobic pocket that is accessible from the lipid bilayer.[61] Interestingly, these ligand-gated ion channels are homolog to the nicotinic acetylcholine receptor, whose electrophysiological activity is reduced by xenon and nitrous oxide.[14] Taken together, these data indicated that the pressures and models used herein are relevant to the study of the mechanisms of clinical anesthesia.

We found that hydrophobicity of the gas binding sites has a screening effect on xenon and nitrous oxide binding, with a threshold value of 83% beyond which and below which xenon and nitrous oxide binds preferentially compared to each other. Xenon that is more polarizable than nitrous oxide tends to prefer very hydrophobic environment while nitrous oxide, which has a dipolar moment, tends to prefer less hydrophobic environment (table 1). In addition, we found that volume, but not hydrophobicity, was further significantly correlated to xenon and nitrous oxide occupancy of the gas binding sites. This suggests that, despite the threshold effect of hydrophobicity in gas binding, volume but not hydrophobicity plays a major role in the degree of gas binding sites' occupancy. Also, we found that occupancy of the gas binding sites by xenon and nitrous oxide was significantly better correlated to the product of hydrophobicity by volume and to the ratio of hydrophobicity to volume, respectively. This indicates that hydrophobicity and volume are binding parameters that complement and oppose each other's effects to determine, respectively, xenon and nitrous oxide occupancy of the gas binding sites.

Alternatively, in line with the well-known Meyer–Overton rule of a high correlation between anesthetic potency and solubility in lipids, we found that the ratio of occupancy of xenon to nitrous oxide was significantly correlated to hydrophobicity of the gas binding sites. In addition, we further found that the mean ratio of occupancy of xenon to nitrous oxide decreased with pressure from 10 to 30 bar, a result consistent with previous studies in rodents that also showed a reduction of the ratio of the *in vivo* effects of these gases from low gas pressures (concentrations) producing narcosis to higher gas pressures producing anesthesia.[2,19,62–66] Together these data indicate with little doubt that xenon and nitrous oxide would act weakly at multiple proteins rather than strongly at specific targets to induce their narcotic and anesthetic effects. This does not preclude, however, that among the multiple target proteins bound by these gases, some of them could play a preponderant role in some particular effect of these gases, for example, the neuroprotective effects of xenon and nitrous oxide that are thought to result largely from their antagonistic properties at the *N*-methyl-D-aspartate glutamatergic receptor whose overactivation is well known to be involved in neuronal death.[2–4,6,7,9,11,13,67–69]

Whether gas binding to proteins within internal cavities, thought to be crucial for conformational flexibility and domain motion,[70,71] or solvent-accessible pockets actually disturbs protein and cell functions is a major question. We recently showed that the ability of xenon and nitrous oxide to bind to urate oxidase disturbs the enzymatic activity of this globular protein.[18,72] Likewise, we further showed that xenon inhibited the catalytic activity of elastase by binding to its active site[51] and demonstrated that xenon and nitrous oxide disrupt in a concentration-dependent manner both the catalytic and thrombolytic activities of tissue-type plasminogen activator,[15,17] a serine protease whose human recombinant form is the only approved therapy for acute ischemic stroke. This agrees with studies that have shown that anesthetic binding to proteins leads to an increase in

Table 1. Physicochemical Properties of Xenon and Nitrous Oxide

Gas	No. of Electrons	Volume, Å^3	Molecular Mass, g/mol	Polarizability, Å^3	Dipole Moment	Blood/Gas Partition Coefficient	Olive Oil/ Gas Partition Coefficient	MAC in Humans, %
Xe	54	42.2	131	4.04	0	0.47	1.4	71
N_2O	22	84.1	44	3.22	0.17	0.14	1.9	105

MAC = minimal alveolar anesthetic concentration; N_2O = nitrous oxide; Xe = xenon.

protein stability[73–75] and to a reduction of kinetics in channel receptors[76] and provides evidence that gas binding to proteins may actually disturb protein and cell functions.

The Meyer–Overton rule has been often used to infer mechanistic models or hypotheses of general narcosis and anesthesia. Particularly, probably due to the use of olive oil or benzene as models to assess solubility in lipids of general anesthetics, the binding sites of general anesthetics and inert gases are often thought to be highly hydrophobic sites. Also, due to the limited number of exceptions to the Meyer–Overton rule, hydrophobicity is often considered as the preponderant binding parameter involved in the processes of gas binding to proteins. By contrast, here we show that (1) xenon and nitrous oxide bound preferentially to hydrophobic sites of high and mild hydrophobicity, respectively; (2) hydrophobicity, in contrast with volume, did not play a significant role in the degree of occupancy of the gas-binding sites by xenon or nitrous oxide; and (3) hydrophobicity is a good predictor of the ratio of the gas binding site occupancy of xenon to nitrous oxide. Taken together, these data demonstrate that xenon and nitrous oxide obey different binding mechanisms, a finding that in turn argues against all unitary hypotheses of narcosis and anesthesia and further indicates that the Meyer–Overton rule, which is often overinterpreted particularly in the field of undersea physiology and medicine, should only be used in its restricted sense of a high correlation between anesthetic potency and solubility in lipids of general anesthetics.

Also, it is noteworthy from this study that both xenon and nitrous oxide bound to binding sites that were either empty or filled with a water molecule (thereby taking the place of the water molecule). Although all (except one) of these binding sites filled with a water molecule were experimental artefacts located at crystallographic interfaces that were therefore not taken into account for data analysis, the fact that xenon and nitrous oxide bound to these binding sites should be considered with interest in future studies since recent data in membrane proteins have reported anesthetic binding in binding sites containing water.[59–61,77] Particularly, it would be of interest to investigate whether our findings in regard to the respective role of hydrophobicity and volume in gas binding to proteins would also apply to binding sites filled with a water molecule.

In conclusion, the present crystallography study provides evidence that the mechanisms of gas binding to proteins and therefore of general anesthesia may no longer be regarded as the result from the sole ability of the general anesthetics to bind to hydrophobic sites according to their solubility in lipids. Also and importantly, as suggested previously for halogenated compounds[78,79] and recently in mutation studies for xenon,[80] our findings strongly support that the mechanisms of gas binding to proteins should be considered as the result of an interaction between a drug ligand and a receptor like in classical pharmacology, that is, as the ability of a drug ligand (here, a gas) to bind to a receptor (a hydrophobic pocket or cavity) and the reciprocal ability of this receptor to bind the drug ligand in a fully reversible manner. With no doubt, such complex mechanisms may explain a number of alterations and exceptions to the Meyer–Overton rule of a high correlation between anesthetic potency and solubility in lipids of general anesthetics, such as the virtual lack of narcotic effect of helium and the so-called nonimmobilizers, which are large inhalational anesthetic-like alkanes.[53,81]

Acknowledgments

The authors gratefully thank Bertrand Castro, Ph.D., D.Sc., and Mohamed El Hajji, Ph.D. (Sanofi-Aventis, Montpellier, France), for their generous gifts of urate oxidase and Hassan Belhari, Ph.D., D.Sc., from the European Molecular Biology Laboratory (Grenoble, France), Gavin Fox, Ph.D., from the European Synchrotron Radiation Facility (Grenoble, France), Jean-Luc Ferrer, Ph.D., D.Sc., and Michel Pirrochi, Ph.D., from the Institut de Biologie Structurale (Grenoble, France), and the staff members of the BM14, BM16, and BM30A beamlines at the European Synchrotron Radiation Facility for their technical help and assistance.

This research was supported by the Centre National de la Recherche Scientifique (Paris, France), the University of Caen Basse Normandie (Caen, France), and the University Paris-Descartes (Paris, France).

Competing Interests

Guillaume Marassio was supported by a grant from the Ministère de l'Education et de la Recherche (Paris, France). The other authors declare no competing interests.

Correspondence

Address correspondence to Dr. Abraini or Dr. Colloc'h: Université de Caen-Basse-Normandie, 14000 Caen, France. jh.abraini@gmail.com or colloch@cyceron.fr. Information on purchasing reprints may be found at www.anesthesiology.org or on the masthead page at the beginning of this issue. Anesthesiology's articles are made freely accessible to all readers, for personal use only, 6 months from the cover date of the issue.

References

1. Cullen SC, Gross EG: The anesthetic properties of xenon in animals and human beings, with additional observations on krypton. Science 1951; 113:580–2

2. David HN, Leveille F, Chazalviel L, MacKenzie ET, Buisson A, Lemaire M, Abraini JH: Reduction of ischemic brain damage by nitrous oxide and xenon. J Cereb Blood Flow Metab 2003; 23:1168–73
3. David HN, Haelewyn B, Rouillon C, Lecoq M, Chazalviel L, Apiou G, Risso JJ, Lemaire M, Abraini JH: Neuroprotective effects of xenon: A therapeutic window of opportunity in rats subjected to transient cerebral ischemia. FASEB J 2008; 22:1275–86
4. Dingley J, Tooley J, Porter H, Thoresen M: Xenon provides short-term neuroprotection in neonatal rats when administered after hypoxia-ischemia. Stroke 2006; 37:501–6
5. Fenster MN: Nitrous oxide as an inhalation anesthetic. J Med Soc N J 1951; 48:281
6. Haelewyn B, David HN, Rouillon C, Chazalviel L, Lecocq M, Risso JJ, Lemaire M, Abraini JH: Neuroprotection by nitrous oxide: Facts and evidence. Crit Care Med 2008; 36:2651–9
7. Homi HM, Yokoo N, Ma D, Warner DS, Franks NP, Maze M, Grocott HP: The neuroprotective effect of xenon administration during transient middle cerebral artery occlusion in mice. Anesthesiology 2003; 99:876–81
8. Hopkins PM: Nitrous oxide: A unique drug of continuing importance for anaesthesia. Best Pract Res Clin Anaesthesiol 2005; 19:381–9
9. Jevtović-Todorović V, Todorović SM, Mennerick S, Powell S, Dikranian K, Benshoff N, Zorumski CF, Olney JW: Nitrous oxide (laughing gas) is an NMDA antagonist, neuroprotectant and neurotoxin. Nat Med 1998; 4:460–3
10. Jordan BD, Wright EL: Xenon as an anesthetic agent. AANA J 2010; 78:387–92
11. Ma D, Hossain M, Chow A, Arshad M, Battson RM, Sanders RD, Mehmet H, Edwards AD, Franks NP, Maze M: Xenon and hypothermia combine to provide neuroprotection from neonatal asphyxia. Ann Neurol 2005; 58:182–93
12. David HN, Ansseau M, Lemaire M, Abraini JH: Nitrous oxide and xenon prevent amphetamine-induced carrier-mediated dopamine release in a memantine-like fashion and protect against behavioral sensitization. Biol Psychiatry 2006; 60:49–57
13. Franks NP, Dickinson R, de Sousa SL, Hall AC, Lieb WR: How does xenon produce anaesthesia? Nature 1998; 396:324
14. Yamakura T, Harris RA: Effects of gaseous anesthetics nitrous oxide and xenon on ligand-gated ion channels. Comparison with isoflurane and ethanol. Anesthesiology 2000; 93:1095–101
15. David HN, Haelewyn B, Risso JJ, Colloc'h N, Abraini JH: Xenon is an inhibitor of tissue-plasminogen activator: Adverse and beneficial effects in a rat model of thromboembolic stroke. J Cereb Blood Flow Metab 2010; 30:718–28
16. Gruss M, Bushell TJ, Bright DP, Lieb WR, Mathie A, Franks NP: Two-pore-domain K+ channels are a novel target for the anesthetic gases xenon, nitrous oxide, and cyclopropane. Mol Pharmacol 2004; 65:443–52
17. Haelewyn B, David HN, Colloc'h N, Colomb DG Jr, Risso JJ, Abraini JH: Interactions between nitrous oxide and tissue plasminogen activator in a rat model of thromboembolic stroke. Anesthesiology 2011; 115:1044–53
18. Marassio G, Prangé T, David HN, Santos JS, Gabison L, Delcroix N, Abraini JH, Colloc'h N: Pressure-response analysis of anesthetic gases xenon and nitrous oxide on urate oxidase: A crystallographic study. FASEB J 2011; 25:2266–75
19. Colloc'h N, Sopkova-de Oliveira Santos J, Retailleau P, Vivarès D, Bonneté F, Langlois d'Estainto B, Gallois B, Brisson A, Risso JJ, Lemaire M, Prangé T, Abraini JH: Protein crystallography under xenon and nitrous oxide pressure: Comparison with in vivo pharmacology studies and implications for the mechanism of inhaled anesthetic action. Biophys J 2007; 92:217–24
20. Hayakawa N, Kasahara T, Hasegawa D, Yoshimura K, Murakami M, Kouyama T: Effect of xenon binding to a hydrophobic cavity on the proton pumping cycle in bacteriorhodopsin. J Mol Biol 2008; 384:812–23
21. Moschetti T, Mueller U, Schulze J, Brunori M, Vallone B: The structure of neuroglobin at high Xe and Kr pressure reveals partial conservation of globin internal cavities. Biophys J 2009; 97:1700–8
22. Olia AS, Casjens S, Cingolani G: Structural plasticity of the phage P22 tail needle gp26 probed with xenon gas. Protein Sci 2009; 18:537–48
23. Prangé T, Schiltz M, Pernot L, Colloc'h N, Longhi S, Bourguet W, Fourme R: Exploring hydrophobic sites in proteins with xenon or krypton. Proteins 1998; 30:61–73
24. Quillin ML, Breyer WA, Griswold IJ, Matthews BW: Size versus polarizability in protein-ligand interactions: Binding of noble gases within engineered cavities in phage T4 lysozyme. J Mol Biol 2000; 302:955–77
25. Sauer O, Roth M, Schirmer T, Rummel G, Kratky C: Low-resolution detergent tracing in protein crystals using xenon or krypton to enhance X-ray contrast. Acta Crystallogr D Biol Crystallogr 2002; 58(Part 1):60–9
26. Schiltz M, Fourme R, Broutin I, Prangé T: The catalytic site of serine proteinases as a specific binding cavity for xenon. Structure 1995; 3:309–16
27. Colloc'h N, el Hajji M, Bachet B, L'Hermite G, Schiltz M, Prangé T, Castro B, Mornon JP: Crystal structure of the protein drug urate oxidase-inhibitor complex at 2.05 A resolution. Nat Struct Biol 1997; 4:947–52
28. Vaney MC, Broutin I, Retailleau P, Douangamath A, Lafont S, Hamiaux C, Prangé T, Ducruix A, Riès-Kautt M: Structural effects of monovalent anions on polymorphic lysozyme crystals. Acta Crystallogr D Biol Crystallogr 2001; 57(Part 7):929–40
29. Kendrew JC, Dickerson RE, Strandberg BE, Hart RG, Davies DR, Phillips DC, Shore VC: Structure of myoglobin: A three-dimensional Fourier synthesis at 2 A. resolution. Nature 1960; 185:422–7
30. Burmester T, Weich B, Reinhardt S, Hankeln T: A vertebrate globin expressed in the brain. Nature 2000; 407:520–3
31. Sun Y, Jin K, Mao XO, Zhu Y, Greenberg DA: Neuroglobin is up-regulated by and protects neurons from hypoxic-ischemic injury. Proc Natl Acad Sci U S A 2001; 98:15306–11
32. Sun Y, Jin K, Peel A, Mao XO, Xie L, Greenberg DA: Neuroglobin protects the brain from experimental stroke in vivo. Proc Natl Acad Sci U S A 2003; 100:3497–500
33. Vallone B, Nienhaus K, Brunori M, Nienhaus GU: The structure of murine neuroglobin: Novel pathways for ligand migration and binding. Proteins 2004; 56:85–92
34. Schiltz M, Prangé T, Fourme R: On the preparation and x-ray data collection of isomorphous xenon derivatives. J Appl Cryst 1994; 27:950–60
35. Schiltz M, Fourme R, Prangé T: Use of noble gases xenon and krypton as heavy atoms in protein structure determination. Methods Enzymol 2003; 374:83–119
36. Otwinowski Z, Minor W: Processing of X-ray diffraction data collected in the oscillation mode. Methods Enzymol 1997; 276:307–26
37. Leslie AG: The integration of macromolecular diffraction data. Acta Crystallogr D Biol Crystallogr 2006; 62(Part 1):48–57
38. Murshudov GN, Vagin AA, Dodson EJ: Refinement of macromolecular structures by the maximum-likelihood method. Acta Crystallogr D Biol Crystallogr 1997; 53(Part 3):240–55
39. Collaborative Computational Project 4: The CCP4 suite: Programs for protein crystallography. Acta Crystallogr D Biol Crystallogr 1994; 50:760–3
40. Arcovito A, Benfatto M, Cianci M, Hasnain SS, Nienhaus K, Nienhaus GU, Savino C, Strange RW, Vallone B, Della Longa S: X-ray structure analysis of a metalloprotein with enhanced active-site resolution using in situ x-ray absorption near edge structure spectroscopy. Proc Natl Acad Sci U S A 2007; 104:6211–6

41. Emsley P, Cowtan K: Coot: Model-building tools for molecular graphics. Acta Crystallogr D Biol Crystallogr 2004; 60(12, Part 1):2126–32
42. Dundas J, Ouyang Z, Tseng J, Binkowski A, Turpaz Y, Liang J: CASTp: Computed atlas of surface topography of proteins with structural and topographical mapping of functionally annotated residues. Nucleic Acids Res 2006; 34(Web Server issue):W116–8
43. Vitali J, Robbins AH, Almo SC, Tilton RF: Using xenon as a heavy atom for determining phases in sperm whale metmyoglobin. J Appl Cryst 1991; 24:931–5
44. Mueller-Dieckmann C, Polentarutti M, Djinovic Carugo K, Panjikar S, Tucker PA, Weiss MS: On the routine use of soft X-rays in macromolecular crystallography. Part II. Data-collection wavelength and scaling models. Acta Crystallogr D Biol Crystallogr 2004; 60(Part 1):28–38
45. Takeda K, Miyatake H, Park SY, Kawamoto M, Kamiya N, Miki K: Multi-wavelength anomalous diffraction method for I and Xe atoms using ultra-high-energy X-rays from SPring-8. J Appl Crystallogr 2004; 37:925–33
46. Savino C, Miele AE, Draghi F, Johnson KA, Sciara G, Brunori M, Vallone B: Pattern of cavities in globins: The case of human hemoglobin. Biopolymers 2009; 91:1097–107
47. Schoenborn BP, Watson HC, Kendrew JC: Binding of xenon to sperm whale myoglobin. Nature 1965; 207:28–30
48. Tilton RF Jr, Kuntz ID Jr, Petsko GA: Cavities in proteins: Structure of a metmyoglobin-xenon complex solved to 1.9 A. Biochemistry 1984; 23:2849–57
49. Vallone B, Nienhaus K, Matthes A, Brunori M, Nienhaus GU: The structure of carbonmonoxy neuroglobin reveals a heme-sliding mechanism for control of ligand affinity. Proc Natl Acad Sci U S A 2004; 101:17351–6
50. Abbruzzetti S, Faggiano S, Bruno S, Spyrakis F, Mozzarelli A, Dewilde S, Moens L, Viappiani C: Ligand migration through the internal hydrophobic cavities in human neuroglobin. Proc Natl Acad Sci U S A 2009; 106:18984–9
51. Colloc'h N, Marassio G, Prangé T: Protein-noble gas interactions investigated by crystallography on three enzymes. Implication on anesthesia and neuroprotection mechanisms, Current Trends in X-ray Crystallography. Edited by Chandrasekaran A. Rijeka, Croatia, InTech, 2010, pp 285–308
52. Miller KW: The nature of sites of general anaesthetic action. Br J Anaesth 2002; 89:17–31
53. Dodson BA, Furmaniuk ZW Jr, Miller KW: The physiological effects of hydrostatic pressure are not equivalent to those of helium pressure on *Rana pipiens*. J Physiol 1985; 362:233–44
54. Girard E, Marchal S, Perez J, Finet S, Kahn R, Fourme R, Marassio G, Dhaussy AC, Prangé T, Giffard M, Dulin F, Bonneté F, Lange R, Abraini JH, Mezouar M, Colloc'h N: Structure-function perturbation and dissociation of tetrameric urate oxidase by high hydrostatic pressure. Biophys J 2010; 98:2365–73
55. Abraini JH, Tomei C, Rostain JC: Quantitative study of behavioral disturbances in rats exposed to high pressure. Ann Physiol Anthropol 1991; 10:183–8
56. Miller KW: The opposing physiological effects of high pressures and inert gases. Fed Proc 1977; 36:1663–7
57. Oakley S, Vedula LS, Bu W, Meng QC, Xi J, Liu R, Eckenhoff RG, Loll PJ: Recognition of anesthetic barbiturates by a protein binding site: A high resolution structural analysis. PLoS One 2012; 7:e32070
58. Vedula LS, Brannigan G, Economou NJ, Xi J, Hall MA, Liu R, Rossi MJ, Dailey WP, Grasty KC, Klein ML, Eckenhoff RG, Loll PJ: A unitary anesthetic binding site at high resolution. J Biol Chem 2009; 284:24176–84
59. Hilf RJ, Dutzler R: X-ray structure of a prokaryotic pentameric ligand-gated ion channel. Nature 2008; 452:375–9
60. Spurny R, Billen B, Howard RJ, Brams M, Debaveye S, Price KL, Weston DA, Strelkov SV, Tytgat J, Bertrand S, Bertrand D, Lummis SC, Ulens C: Multisite binding of a general anesthetic to the prokaryotic pentameric *Erwinia chrysanthemi* ligand-gated ion channel (ELIC). J Biol Chem 2013; 288:8355–64
61. Nury H, Van Renterghem C, Weng Y, Tran A, Baaden M, Dufresne V, Changeux JP, Sonner JM, Delarue M, Corringer PJ: X-ray structures of general anaesthetics bound to a pentameric ligand-gated ion channel. Nature 2011; 469:428–31
62. Koblin DD, Fang Z, Eger EI II, Laster MJ, Gong D, Ionescu P, Halsey MJ, Trudell JR: Minimum alveolar concentrations of noble gases, nitrogen, and sulfur hexafluoride in rats: Helium and neon as nonimmobilizers (nonanesthetics). Anesth Analg 1998; 87:419–24
63. Miller KW, Wilson MW, Smith RA: Pressure resolves two sites of action of inert gases. Mol Pharmacol 1978; 14:950–9
64. Russell GB, Graybeal JM: Direct measurement of nitrous oxide MAC and neurologic monitoring in rats during anesthesia under hyperbaric conditions. Anesth Analg 1992; 75:995–9
65. Russell GB, Graybeal JM: Differences in anesthetic potency between Sprague-Dawley and Long-Evans rats for isoflurane but not nitrous oxide. Pharmacology 1995; 50:162–7
66. Russell GB, Graybeal JM: Nonlinear additivity of nitrous oxide and isoflurane potencies in rats. Can J Anaesth 1998; 45(5, Part 1):466–70
67. Abraini JH, David HN, Lemaire M: Potentially neuroprotective and therapeutic properties of nitrous oxide and xenon. Ann N Y Acad Sci 2005; 1053:289–300
68. Banks P, Franks NP, Dickinson R: Competitive inhibition at the glycine site of the N-methyl-D-aspartate receptor mediates xenon neuroprotection against hypoxia-ischemia. Anesthesiology 2010; 112:614–22
69. Harris K, Armstrong SP, Campos-Pires R, Kiru L, Franks NP, Dickinson R: Neuroprotection against traumatic brain injury by xenon, but not argon, is mediated by inhibition at the N-methyl-D-aspartate receptor glycine site. Anesthesiology 2013; 119:1137–48
70. Hubbard SJ, Argos P: Cavities and packing at protein interfaces. Protein Sci 1994; 3:2194–206
71. Hubbard SJ, Argos P: A functional role for protein cavities in domain: Domain motions. J Mol Biol 1996; 261:289–300
72. Colloc'h N, Prangé T: Functional relevance of the internal hydrophobic cavity of urate oxidase. FEBS Lett 2014; 588:1715–9
73. Eckenhoff RG, Johansson JS: Molecular interactions between inhaled anesthetics and proteins. Pharmacol Rev 1997; 49:343–67
74. Johansson JS, Zou H, Tanner JW: Bound volatile general anesthetics alter both local protein dynamics and global protein stability. Anesthesiology 1999; 90:235–45
75. Tanner JW, Liebman PA, Eckenhoff RG: Volatile anesthetics alter protein stability. Toxicol Lett 1998; 100–101:387–91
76. Dilger JP, Vidal AM, Mody HI, Liu Y: Evidence for direct actions of general anesthetics on an ion channel protein. A new look at a unified mechanism of action. Anesthesiology 1994; 81:431–42
77. Sauguet L, Howard RJ, Malherbe L, Lee US, Corringer PJ, Harris RA, Delarue M: Structural basis for potentiation by alcohols and anaesthetics in a ligand-gated ion channel. Nat Commun 2013; 4:1697
78. Franks NP, Lieb WR: Do general anaesthetics act by competitive binding to specific receptors? Nature 1984; 310:599–601
79. Franks NP, Lieb WR: Molecular and cellular mechanisms of general anaesthesia. Nature 1994; 367:607–14
80. Armstrong SP, Banks PJ, McKitrick TJ, Geldart CH, Edge CJ, Babla R, Simillis C, Franks NP, Dickinson R: Identification of two mutations (F758W and F758Y) in the *N*-methyl-D-aspartate receptor glycine-binding site that selectively prevent competitive inhibition by xenon without affecting glycine binding. Anesthesiology 2012; 117: 38–47
81. Perouansky M: Non-immobilizing inhalational anesthetic-like compounds. Handb Exp Pharmacol 2008; 182:209–23